Noncoincidence Effect of Vibrational Bands of Methanol/CCl_4 Mixtures and Its Relation with Concentration-Dependent Liquid Structures

Maurizio Musso,[†] Hajime Torii,*[,‡] Paolo Ottaviani,[§] Augustinus Asenbaum,[†] and Maria Grazia Giorgini[§]

Institut für Physik und Biophysik, Universität Salzburg, Hellbrunnerstrasse 34, A-5020 Salzburg, Austria, Department of Chemistry, School of Education, Shizuoka University, 836 Ohya, Shizuoka 422-8529, Japan, and Dipartimento di Chimica Fisica ed Inorganica, Università di Bologna, Viale del Risorgimento 4, I-40136 Bologna, Italy

Received: June 18, 2002; In Final Form: August 7, 2002

The concentration dependence of the Raman noncoincidence effect (NCE) of the C−O and O−H stretching bands of methanol is investigated in methanol/CCl_4 mixtures in the range of $1.0 \geq x_m \geq 0.1$, where x_m is the mole fraction of methanol, by performing Raman spectroscopic measurements and molecular dynamics (MD) simulations. Band asymmetry observed for both bands is carefully taken into account. The experimental and simulation results are in satisfactory agreement with each other. For the C−O stretching band, it is observed that the magnitude of the negative NCE gets larger upon dilution in CCl_4 down to $x_m \sim 0.2$, contrary to the expectation of becoming smaller from simple guess that the NCE arises from intermolecular vibrational resonant interactions between methanol molecules, which, on average, get separated from each other upon dilution. For the O−H stretching band, the magnitude of the positive NCE remains almost the same upon dilution down to $x_m \sim 0.3$. These apparently peculiar experimental results are reasonably explained by the MD simulations on the basis of the transition dipole coupling (TDC) mechanism of intermolecular resonant vibrational interactions and the simulated hydrogen-bonded liquid structures. In the case of the C−O stretching band, the negative NCE arises mainly from positive vibrational coupling between hydrogen-bonded pairs of molecules, which is partially canceled by negative vibrational coupling between molecules in different hydrogen-bonded chains. In the case of the O−H stretching band, the positive NCE arises predominantly from negative vibrational coupling within hydrogen-bonded chains. As a result, a locally anisotropic change in the liquid structure that occurs upon dilution, in which, around each molecule, intermolecular distances do not change very much along hydrogen-bond directions but do change significantly in other directions, gives rise to the apparently peculiar behavior of the NCE described above.

1. Introduction

The so-called Raman noncoincidence effect (NCE) observed in a molecular liquid is the phenomenon that the frequency positions of the isotropic and anisotropic components of the band profile of a Raman-active vibrational mode do not coincide.[1] NCE arises from intermolecular resonant vibrational interactions between neighboring molecules that give rise to delocalization of vibrational modes. It is particularly manifest in polar liquids and is influenced by the molecular local order in the liquid itself.[2−4]

Neat liquid methanol shows NCE both in the C−O stretching [ν(C−O)] region at around 1030 cm^{-1} and in the O−H stretching [ν(O−H)] region at around 3300−3400 cm^{-1}.[5,6] A very remarkable fact is that the ν(C−O) band of methanol has a *negative* NCE[7−9] [$NCE_p \approx -5.3(5)$ cm^{-1},[8] where NCE_p is the value of NCE determined from the peak frequency positions, defined as $NCE_p = \tilde{\nu}_{peak,ani} - \tilde{\nu}_{peak,iso}$], while the ν(O−H) band of methanol has a *positive* NCE[9,10] [$NCE_p \approx +85(5)$ cm^{-1} [10]].

Several molecular dynamics (MD) simulations of neat liquid methanol have been carried out with various intermolecular potentials to deepen the knowledge of its structural and thermophysical properties.[11−16] It has been clarified that the majority of molecules in liquid methanol have two hydrogen bonds, and the liquid is basically made up of winding linear chains of hydrogen-bonded molecules. The number of monomers per chain at room temperature is found to be typically between 5 and 20, depending on the intermolecular potential used, although the presence of a nonnegligible degree of cross bonding makes it impossible to speak unambiguously of a mean chain length (see also the discussion in ref 17).

Monte Carlo (MC) and molecular dynamics (MD) simulations of the NCE of the ν(C−O) and ν(O−H) bands of neat liquid methanol[18,19] have successfully reproduced the experimental NCE values observed in the neat liquid. They have offered, on the basis of the simulated liquid structure and the transition−dipole coupling (TDC) mechanism as the mechanism of intermolecular resonant vibrational interaction, a complete explanation of the opposite signs observed for the NCE in its ν(C−O) and ν(O−H) bands: (a) the vibrational interactions between O−H oscillators within each hydrogen-bonded chain (intrachain O−H coupling) account for the major part of the positive NCE of the ν(O−H) band; (b) the vibrational interactions between C−O oscillators of hydrogen-bonded pairs of molecules induce a negative NCE of the ν(C−O) band (roughly speaking, intrachain C−O coupling), which is partially canceled

* Author to whom correspondence should be addressed. Telephone: +81-54-238-4624. Fax: +81-54-237-3354. E-mail: torii@ed.shizuoka.ac.jp.
[†] Universität Salzburg.
[‡] Shizuoka University.
[§] Università di Bologna.

10.1021/jp021440a CCC: $22.00
Published on Web 10/01/2002

by the contribution from the vibrational interactions between C−O oscillators of non-hydrogen-bonded pairs (roughly speaking, interchain C−O coupling). The negative NCE of the ν(C−O) band of methanol is opposed to the positive NCE observed for the C═O stretching band of acetone. In fact, the liquid structure is mainly determined by hydrogen-bonding interactions in the former and by dipolar interactions in the latter, whereas the intermolecular resonant interactions among vibrational modes are dipolar (TDC) in both liquids.[18]

The expected effect of chemical or isotopic dilution on the NCE of a polar non-hydrogen-bonding solute in a nonpolar solvent is, in ideal cases, a gradual decrease of the magnitude of NCE as the interacting molecules get separated from each other, until it eventually vanishes.[4] The purely dipolar nature of the intermolecular interactions governing the local molecular organization of the solute in a nonpolar solvent is considered to be the origin of this effect. The Raman spectroscopic and computer simulation results of our previous dilution studies on the C═O stretching band of acetone[20−22] and *N*,*N*-dimethylformamide (DMFA)[23] conform to this expectation. The present work is, on one hand, an experimental extension of our former NCE studies on dipolar liquids diluted in CCl_4 (as a nonpolar solvent) to binary mixtures containing a more complex, polar, and *hydrogen-bonding* liquid, which is methanol in the present case. At the same time it is an extension of the MD simulation procedure already used for the NCE of neat methanol[18,19] to that of methanol diluted in CCl_4.

In ref 9 it was reported that the magnitude of the negative NCE (evaluated as the difference in peak frequencies, NCE_p) of the ν(C−O) band of methanol increases upon dilution in CCl_4. Generally, much care should be taken for a meaningful interpretation of the observed concentration dependence of NCE_p, because the band shape of the isotropic and anisotropic component has an intrinsic asymmetry in the neat liquid, caused by resonant intermolecular interactions,[24] which changes with dilution due to progressive removal of the resonant interaction and due to the influence of concentration fluctuations.[24,25] This leads to different behavior of peak frequency $\tilde{\nu}_{peak}$ and first moment $M_1 = \int\tilde{\nu}\cdot I(\tilde{\nu} - \tilde{\nu}_0)\, d\tilde{\nu} / \int I(\tilde{\nu} - \tilde{\nu}_0)\, d\tilde{\nu}$ upon dilution (these two quantities being equivalent only for symmetric bands).[20−23] Since theoretical formulations deal with a moment expansion of an intensity distribution, the theoretical and experimental results can only be safely compared if one considers the first moments M_1.

The purpose of the present study is 3-fold: (1) to reveal the spectral changes that occur upon dilution of liquid methanol in CCl_4, (2) to correlate these observed spectral changes with local liquid structures (predominantly influenced by hydrogen bonding between molecules) by means of simulations of vibrational bands using the MD method and the TDC mechanism (the MD/TDC method), and (3) to compare the results of the present study, obtained with careful analysis of the considerable asymmetry of the ν(C−O) and ν(O−H) band profiles of methanol, with those reported by other groups.[7−10,26]

2. Experimental and Computational Procedures

A. Experimental. The chemical mixtures were prepared with UV-spectroscopy grade chemicals used without further purification. The mixtures were spectroscopically analyzed in quadratic cells at a constant temperature of 293 K. The compositions of the mixtures were set to $x_m = 1.0$, 0.9, 0.8, 0.7, 0.6, 0.5, 0.4, 0.3, 0.2, and 0.1, where x_m is the mole fraction of methanol. In the ν(C−O) region, measurements were also carried out for the mixtures of $x_m = 0.05$, 0.02, and 0.01. For each mixture, the Raman spectra in parallel (VV) and crossed (HV) polarizations for exciting and scattered light were obtained by rotating the polarization of the exciting laser light with the help of a Fresnel rhomb retarder (V or H) and observing the scattered Raman light through a polarizer (V). The depolarization ratio was checked using the standard procedure with liquid CCl_4. The laser used is a single-mode single-frequency Ar^+ laser operating at 514.53 nm and with 200 mW laser light power on the sample. Each mixture was measured in each polarization configuration taking the average of 10 accumulations with integration times between 30 and 600 s for each single accumulation.

In the ν(C−O) region, the Raman light was detected in 90° scattering geometry by a liquid nitrogen cooled CCD camera on a Jobin-Yvon U-1000 spectrometer. The slit width was set to 100 μm, producing a Gaussian slit function with *fwhm* = 0.67 cm^{-1}. To cover the spectral range of 400 cm^{-1} from 820 to 1220 cm^{-1}, with a sampling point distance of 0.19 cm^{-1}, three overlapping spectral regions were necessary. Correction for the instrumentally influenced intensity distribution was achieved by dividing the spectra with the normalized spectra obtained from a luminescence standard (fluoresceine). The spectra were then spliced together to get the overall spectrum.

In the ν(O−H) region, the Raman light was detected in 180° scattering geometry by a liquid nitrogen cooled CCD camera on a Dilor XY spectrometer with macro entrance. The slit width was set to 200 μm, producing a Gaussian slit function with fwhm = 2.9 cm^{-1}. To cover the spectral range of 1500 cm^{-1} from 2500 to 4000 cm^{-1}, with a sampling point distance of 0.60 cm^{-1}, four spectral regions were necessary, which were spliced together to obtain an overall spectrum. This was corrected for the instrumentally influenced intensity distribution by dividing it with the normalized spectrum obtained from a tungsten bulb as approximated blackbody source.

The band position was calibrated against instrumental frequency instabilities (thermal drifts) with the help of a Neon pen ray lamp, using the Ne I lines at 540.05618 nm for the ν(C−O) band and at 632.81653 nm for the ν(O−H) band, respectively.[27]

B. Observed Data Treatment. The observed spectral profiles were fitted with the help of spectroscopy software routines (GRAMS 5.1). The isotropic spectra were obtained from the VV and HV spectra through the relation $I_{iso} = I_{VV} - {}^4/_3 I_{HV}$, while the HV spectrum directly gives the anisotropic spectrum, $I_{ani} = I_{HV}$. The quality of the fits of the isotropic and anisotropic spectra was checked through the χ^2 value obtained in the least-squares fit and the uncertainties (σ_i) in the positions and areas of the Gauss-Lorentz bands (given by $f(x) = (1 - M)\cdot f_{gauss} + M\cdot f_{lor}$, with f_{gauss} and f_{lor} being the usual Gaussian and Lorentzian functions and M being the Lorentzian fraction) necessary to fit the *whole* spectrum in the 820−1220 or 2500−4000 cm^{-1} region. Since these statistical parameters (χ^2, σ_i) are inversely correlated to the number of Gauss-Lorentz bands used in the fit, we chose this quantity on the basis of the best compromise between χ^2 value and the parameter uncertainties. In the fitting procedure all parameters of the Gauss-Lorentz bands (width, height, position, Lorentzian fraction) were allowed to change. In the 2500−4000 cm^{-1} region, the fitting procedure was done in the following two steps, as the stronger peaks govern the overall fit result because of the signal/noise ratio. First, the dominating symmetric and antisymmetric methyl stretch contributions[5,6] around 3000 cm^{-1} were subtracted from the fitted spectra. Then, the fits were carried out again in a more restricted region between 3000 and 4000 cm^{-1}.

The following quantities were determined for the ν(C−O) and ν(O−H) bands: the peak frequency positions $\tilde{\nu}_{peak,iso}$ and $\tilde{\nu}_{peak,ani}$, the first moments $M_{1,iso}$ and $M_{1,ani}$ over the *whole*

spectral profile of each band, and the full width at half-maximum $\mathrm{fwhm_{iso}}$ and $\mathrm{fwhm_{ani}}$. The NCE has been evaluated as a difference of the peak frequency positions $\mathrm{NCE_p} = \tilde{\nu}_{\mathrm{peak,ani}} - \tilde{\nu}_{\mathrm{peak,iso}}$ as well as that of the first moments $\mathrm{NCE_M} = M_{1,\mathrm{ani}} - M_{1,\mathrm{iso}}$. The uncertainties of all these quantities are given at the 95% confidence level.

All the measurements and the observed data treatments were carried out in Salzburg.

C. MD Simulations. Calculations of vibrational spectra were based on the liquid structures obtained from MD simulations and the TDC mechanism for intermolecular vibrational interactions. The MD simulations were performed using polarizable potential functions of methanol[28] and CCl_4[29] for mixtures of composition in the range of $1.0 \geq x_m \geq 0.1$.[30] Only intermolecular degrees of freedom were considered. The total number of molecules in the simulation box with *NVT* fixed was $N = 500$, with temperature $T = 293$ K and the molecular volume $v_{\mathrm{MeOH}} = 71.2$ Å^3 and $v_{\mathrm{CCl_4}} = 160.6$ Å^3. The periodic boundary condition was employed. The time step was set to 2 fs. In each simulation, a time interval of over 240 ps was allowed to elapse for reaching thermal equilibrium, then 400 configurations were extracted in the subsequent sampling interval of 200 ps (one every 500 fs) to determine the band profiles. The normal modes of the mixtures were obtained by diagonalizing the F matrix, whose off-diagonal terms were determined by the TDC mechanism.

In the previous MD simulation study on the NCE of neat liquid methanol,[19] a common value of diagonal force constant [$f_{\mathrm{OH}} = 6.75$ mdyn Å^{-1} amu^{-1} for the ν(O−H) mode and $f_{\mathrm{CO}} = 0.627$ mdyn Å^{-1} amu^{-1} for the ν(C−O) mode] were assumed for all the molecules in the liquid. This was considered to be a reasonable approximation because essentially all the molecules in the liquid are hydrogen bonded to other molecules. However, to deal with the effects of dilution in CCl_4, it is necessary to introduce variation of diagonal force constants f with the hydrogen-bonding condition of molecules. Additionally, it is expected that the magnitude of dipole derivative (or transition dipole) of the ν(O−H) mode, $(\partial\mu/\partial Q)_{\mathrm{OH}}$, also depends on the hydrogen-bonding condition of molecules, because it is well-known that the IR intensity (proportional to the square of dipole derivative) of this mode gets significantly larger by forming a hydrogen bond as a proton donor.

To get insight into the variation of these two quantities with hydrogen-bonding condition, ab initio molecular orbital (MO) and density functional (DFT) calculations were carried out for some linear and cyclic clusters of methanol molecules (linear dimer to tetramer and cyclic trimer to hexamer) at the HF, MP2, and B3LYP levels of theory with the 6-31+G** basis set by using the Gaussian 98 program.[31] The calculations suggest that f_{OH} and $(\partial\mu/\partial Q)_{\mathrm{OH}}$ are almost linearly dependent on the hydrogen-bond length $r_{\mathrm{O\cdots H}}$, although the coefficients of the linear dependence vary with the theoretical level, and none of the theoretical levels adopted in the present study seems to be sufficient to provide reasonable values of the coefficients that can be directly used in the simulations. We therefore adjusted the coefficients so that the simulated spectral profiles are in reasonable agreement with the observed ones. We obtained f_{OH} (/mdyn Å^{-1} amu^{-1}) $= 3.095 + 1.960\, r_{\mathrm{O\cdots H}}$ (/Å) and $(\partial\mu/\partial Q)_{\mathrm{OH}}$ (/D Å^{-1} amu$^{-1/2}$) $= 16.149 - 7.335\, r_{\mathrm{O\cdots H}}$ (/Å) for hydrogen-bond donating molecules. Both the coefficients in the former formula were determined rather precisely, since they are sensitive to the location and the overall width of the oligomer ν(O−H) band. The coefficients in the latter formula were derived from those obtained from ab initio MO calculations at the MP2/6-31+G** level with a scale factor of 0.7, which is found to be rather sensitive to the magnitude of the NCE of the oligomer ν(O−H) band. We assumed $f_{\mathrm{OH}} = 7.823$ mdyn Å^{-1} amu^{-1} and $(\partial\mu/\partial Q)_{\mathrm{OH}} = 1.046$ D Å^{-1} amu$^{-1/2}$ for molecules without hydrogen-bond donating O−H group.[32]

The Raman tensor of the ν(O−H) mode was assumed to be axially symmetric with respect to the OH bond, and with the same magnitude and depolarization ratio (0.167) for all the molecules. In fact, the spectral profiles do not depend on the assumed value of depolarization ratio as far as a common value is assumed for all the molecules. Only the relative intensities between the isotropic and anisotropic components depend on this quantity.

The computational procedure described above provided for each liquid sample a set of vibrational frequencies and the isotropic and anisotropic Raman intensities of delocalized normal modes. The overall spectral profiles were then obtained by convoluting these "stick spectra" with appropriate band shape functions. At this stage, we have to deal with the difference in the intrinsic bandwidth of the ν(O−H) mode, which, arising probably from the differences in the vibrational population relaxation and dephasing rates, is expected to depend on the hydrogen-bond condition. We assumed a Gaussian band profile, supposing that the vibrational dephasing of the OH stretching mode is in the slow modulation regime, and set the width as $\mathrm{fwhm_{iso}} = \mathrm{fwhm_{ani}} = 40$ cm^{-1} for each mode of a hydrogen-bond donating molecule, and $\mathrm{fwhm_{iso}} = 6.2$ cm^{-1} and $\mathrm{fwhm_{ani}} = 12.5$ cm^{-1} for that of a molecule without a hydrogen-bond donating O−H group. Each delocalized normal mode of liquids obtained in the simulations generally has contributions from both kinds of molecules. The widths of convoluting band profiles were determined by linear interpolation in this regard.

For the ν(C−O) mode, ab initio MO and DFT calculations for methanol clusters did not suggest linear dependence of f_{CO} and $(\partial\mu/\partial Q)_{\mathrm{CO}}$ on $r_{\mathrm{O\cdots H}}$. However, the behavior of the observed Raman spectra described below in Section 3A suggests that the value of f_{CO} and the depolarization ratio (ρ_{CO}) depend on the hydrogen-bonding condition. We assumed $f_{\mathrm{CO}} = 0.629$ mdyn Å^{-1} amu^{-1} and $\rho_{\mathrm{CO}} = 0.167$ for hydrogen-bond donating molecules, and $f_{\mathrm{CO}} = 0.617$ mdyn Å^{-1} amu^{-1} and $\rho_{\mathrm{CO}} = 0.0$ for molecules without a hydrogen-bond donating O−H group. The higher value of f_{CO} for the former type of molecules is considered to be reasonable, because the so-called "C−O stretching" mode treated in the present study has some contribution of the OH bending vibration, and a higher force constant of this vibration is expected for a hydrogen-bond donating molecule. The value of $\rho_{\mathrm{CO}} = 0.0$ for the latter type of molecules is derived from the observation described below in Section 3A that the observed depolarization ratio of the corresponding Raman band is negligibly small.

The magnitude of the dipole derivative $(\partial\mu/\partial Q)_{\mathrm{CO}} = 1.54$ D Å^{-1} amu$^{-1/2}$, determined from the observed IR intensity,[33] was assumed to be the same for all the molecules, as in the previous MD simulation study for neat liquid methanol.[18,19] The Raman tensor was assumed to be axially symmetric with respect to the CO bond of each molecule, and its magnitude (i.e., Raman intensity) was assumed to be the same for all the molecules. The convoluting functions used to obtain spectral profiles were assumed to be Lorentzian with $\mathrm{fwhm_{iso}} = 4.0$ cm^{-1} and $\mathrm{fwhm_{ani}} = 8.0$ cm^{-1} for each mode of a hydrogen-bond donating molecule, and $\mathrm{fwhm_{iso}} = \mathrm{fwhm_{ani}} = 2.2$ cm^{-1} for that of a molecule without a hydrogen-bond donating O−H group.

All the simulations described above were carried out on NEC SX-5 and Fujitsu VPP5000 supercomputers at the Research

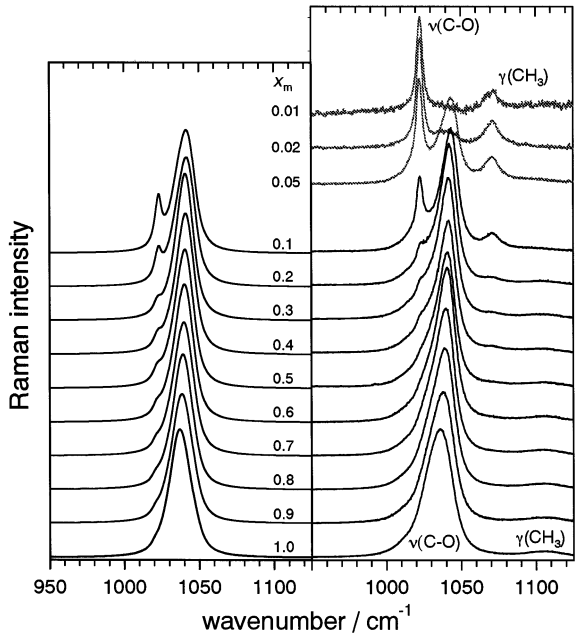

Figure 1. Observed (right) and simulated (left) C−O stretching [ν(C−O)] isotropic Raman bands of methanol in methanol/CCl_4 mixtures at 293 K, where x_m is the mole fraction of methanol. The Raman intensities are normalized relative to their integrated intensities. The in-plane methyl rocking bands [$\gamma(CH_3)$] also appear in this frequency region as indicated.

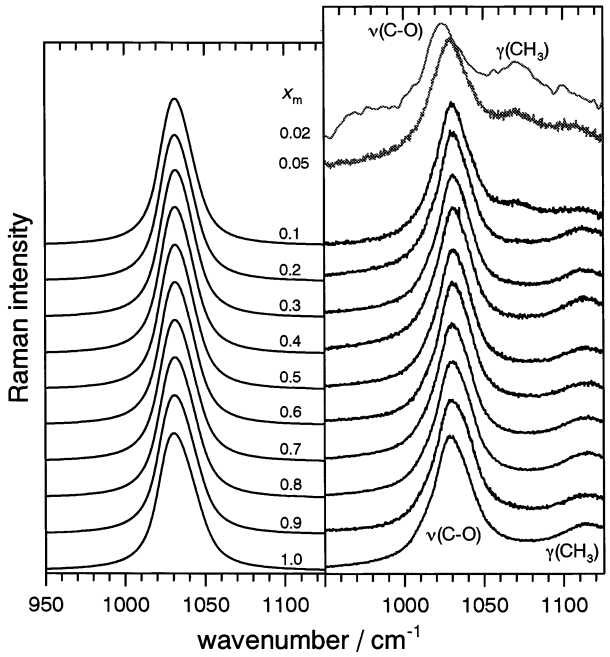

Figure 2. Observed (right) and simulated (left) C−O stretching anisotropic Raman bands of methanol in methanol/CCl_4 mixtures at 293 K. See also the caption for Figure 1.

Center for Computational Science of the Okazaki National Research Institutes, and on a Compaq XP1000 workstation in one of the author's laboratory in Shizuoka.

3. Results and Discussion

A. Spectral Profiles. The concentration dependence of the observed and simulated spectral profiles of the isotropic and anisotropic components of the ν(C−O) Raman band of methanol in methanol/CCl_4 mixtures is shown in Figures 1 and 2, and that of the ν(O−H) Raman band (contributions of the methyl stretching bands subtracted) in Figures 3 and 4. It is seen that progressive dilution of methanol in CCl_4 produces some remarkable changes in the ν(C−O) and ν(O−H) band shapes. As shown below, the origin of the overall spectral profiles may be interpreted with the help of MD simulations of liquids carried out in the present study as well as in previous studies,[13,19,34]

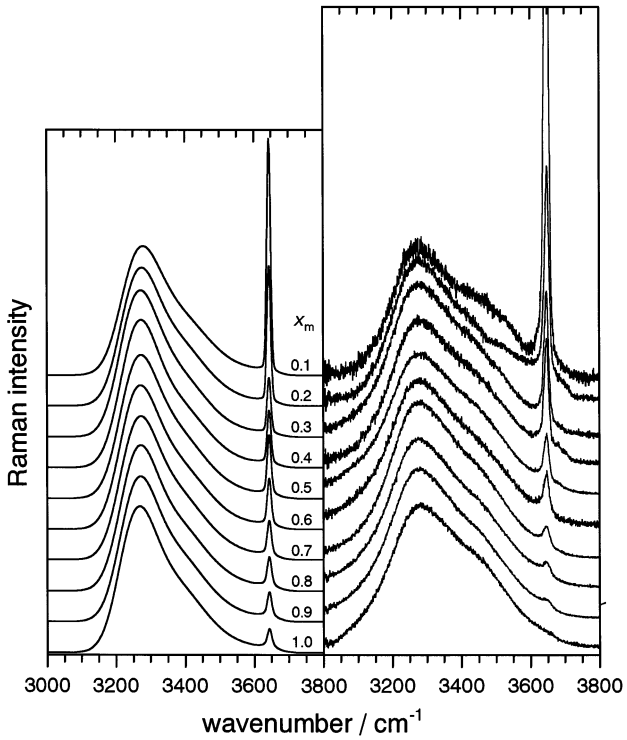

Figure 3. Observed (right) and simulated (left) O−H stretching isotropic Raman bands of methanol in methanol/CCl_4 mixtures at 293 K, where x_m is the mole fraction of methanol. In the observed spectra, the dominating symmetric and asymmetric methyl stretching bands below 3000 cm^{-1} are subtracted, following the band fitting procedure described in the text, to clarify the behavior of the O−H stretching band. The Raman intensities are normalized relative to their integrated intensities.

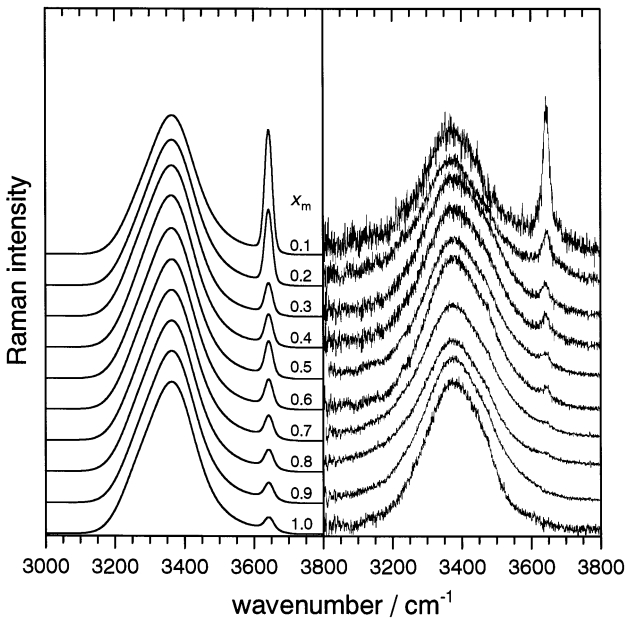

Figure 4. Observed (right) and simulated (left) O−H stretching anisotropic Raman bands of methanol in methanol/CCl_4 mixtures at 293 K. See also the caption for Figure 3.

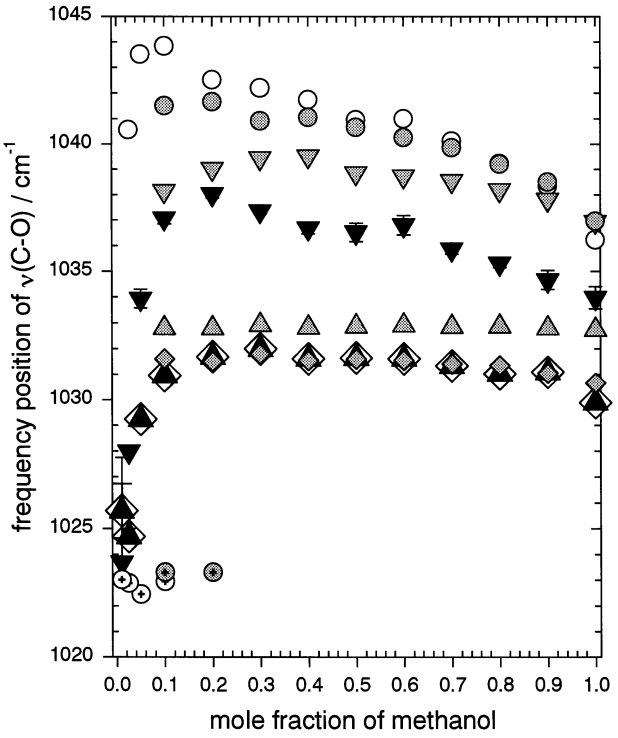

Figure 5. Observed and simulated dependence of the peak frequencies ($\tilde{\nu}_{peak}$) and the first moments (M_1) of the isotropic and anisotropic components of the C−O stretching Raman bands on the mole fraction of methanol in CCl_4 at 293 K. Circle (○): $\tilde{\nu}_{peak,iso}$; diamond (◇): $\tilde{\nu}_{peak,ani}$; downward triangle (▽): $M_{1,iso}$; upward triangle (△): $M_{1,ani}$. The open and filled symbols denote observed values, and the shaded symbols denote simulated values. The symbols with plus (+) at the center denote the values for the end-of-chain band.

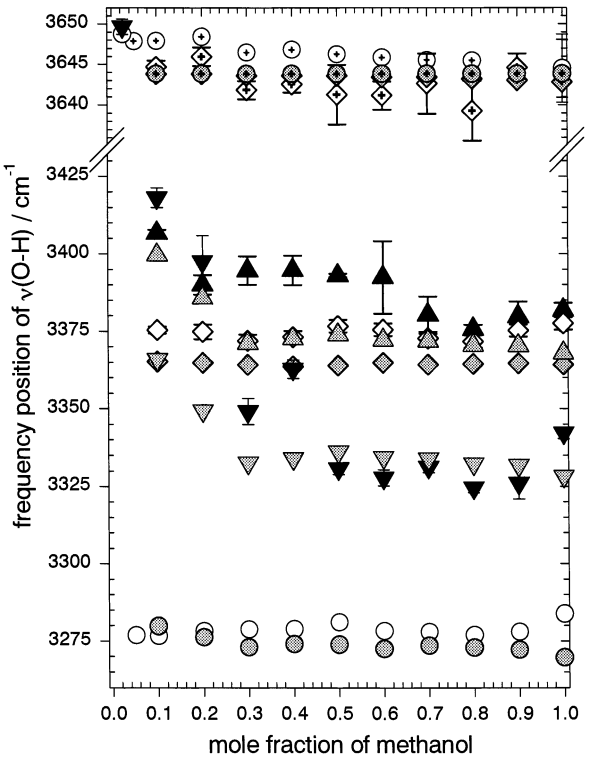

Figure 6. Observed and simulated dependence of the peak frequencies ($\tilde{\nu}_{peak}$) and the first moments (M_1) of the isotropic and anisotropic components of the O−H stretching Raman bands on the mole fraction of methanol in CCl_4 at 293 K. See also the caption for Figure 5.

MO calculations of methanol clusters,[35] and an observed IR spectrum.[36]

In the ν(C−O) region, a broad isotropic Raman band at ∼1035 cm^{-1} [at $x_m = 1.0$, $\tilde{\nu}_{peak,iso}$= 1036.2(1) cm^{-1}, $M_{1,iso}$ = 1034.0(2) cm^{-1}, and $fwhm_{iso}$ = 22.0(2) cm^{-1}] and the corresponding anisotropic Raman band at ∼1030 cm^{-1} [at $x_m = 1.0$, $\tilde{\nu}_{peak,ani} = M_{1,ani}$ = 1029.9(1) cm^{-1} and $fwhm_{ani}$ = 29.4(2) cm^{-1}] are considered to be due to oligomeric units inside hydrogen-bonded chains. Upon dilution, a shoulder on the low-frequency side of the oligomer band in the isotropic Raman spectrum becomes apparent at $x_m \sim 0.3$, which transforms into a well-resolved separate narrow band at $x_m \sim 0.2$ [$\tilde{\nu}_{peak,iso} = M_{1,iso}$ = 1022.8(1) cm^{-1} and $fwhm_{iso}$ = 4.6(2) cm^{-1}]. This band, with an increasing intensity upon dilution, is assigned to solvated molecules without hydrogen-bond donating O−H group located at the chain end (probably including solvated monomers). The lower frequency of this band as compared with the oligomer band is reasonable, as discussed above in Section 2C. There is no anisotropic Raman band regarded as a counterpart of this isotropic Raman band except in a very dilute solution (x_m = 0.02), indicating that the depolarization ratio of this band is very small. The intensity of the oligomer band decreases upon dilution, until it vanishes at high dilutions, $x_m \leq 0.02$.

The concentration dependence of the peak frequencies $\tilde{\nu}_{peak}$ (both for the oligomer band and the end-of-chain band) and the first moments M_1 of the ν(C−O) isotropic and anisotropic Raman band profiles is shown in Figure 5. It is seen that the isotropic component of the oligomer band shifts to higher frequencies upon dilution down to $x_m = 0.2$ compared to the position in neat liquid methanol. Upon further dilution, a remarkable decrease of $M_{1,iso}$ is observed due to the increasing intensity of the end-of-chain ν(C−O) band. The anisotropic component shows only a slight increase in frequency upon dilution down to $x_m = 0.2$. Below this concentration there is a shift to a value close to $M_{1,iso}$.

As shown in Figure 5, the MD simulation reproduces the observed concentration dependence. It may be said that the agreement is good for the peak frequencies and fair for the first moments.

In the ν(O−H) region, a broad isotropic Raman band with an asymmetric shape at ∼3300 cm^{-1} [at $x_m = 1.0$, $\tilde{\nu}_{peak,iso}$ = 3283(2) cm^{-1}, $M_{1,iso}$ = 3341(1) cm^{-1}, and $fwhm_{iso}$ = 330(20) cm^{-1}] and the corresponding anisotropic Raman band at ∼3380 cm^{-1} [at $x_m = 1.0$, $\tilde{\nu}_{peak,ani}$ = 3377(2) cm^{-1}, $M_{1,ani}$ = 3381(3) cm^{-1}, and $fwhm_{ani}$ = 213(20) cm^{-1}] are due to oligomeric units inside hydrogen-bonded chains, just as the ν(C−O) band at ∼1030 cm^{-1} discussed above. Upon dilution in CCl_4, another narrower band at ∼3650 cm^{-1} increases in intensity in the isotropic and anisotropic Raman spectra. At the noise level obtained here, this band appears to be symmetric, and hence the peak frequency coincides with the first moment [at x_m = 1.0, $\tilde{\nu}_{peak,iso} = M_{1,iso}$ = 3644.5(3.9) cm^{-1}]. It is assigned to solvated molecules without hydrogen-bond donating O−H group located at the chain end, including solvated monomers.[7,9,10,26]

The concentration dependence of the peak frequencies and the first moments of the ν(O−H) isotropic and anisotropic Raman band profiles is shown in Figure 6. It is seen that the peak frequency (as well as the band shape in Figure 3) of the oligomer ν(O−H) isotropic Raman band does not appreciably change with dilution, while starting at $x_m \sim 0.5$ the first moment $M_{1,iso}$ gradually increases due to the increasing intensity of the end-of-chain ν(O−H) band at ∼3650 cm^{-1}. The latter gradually shifts from 3643.8(1.0) cm^{-1} (at $x_m = 0.9$) to 3647.9(4) cm^{-1} (at $x_m = 0.1$) upon dilution with narrowing bandwidth [$fwhm_{iso}$ = 40 to 15.3(2) cm^{-1}]. Note that in neat liquid methanol only

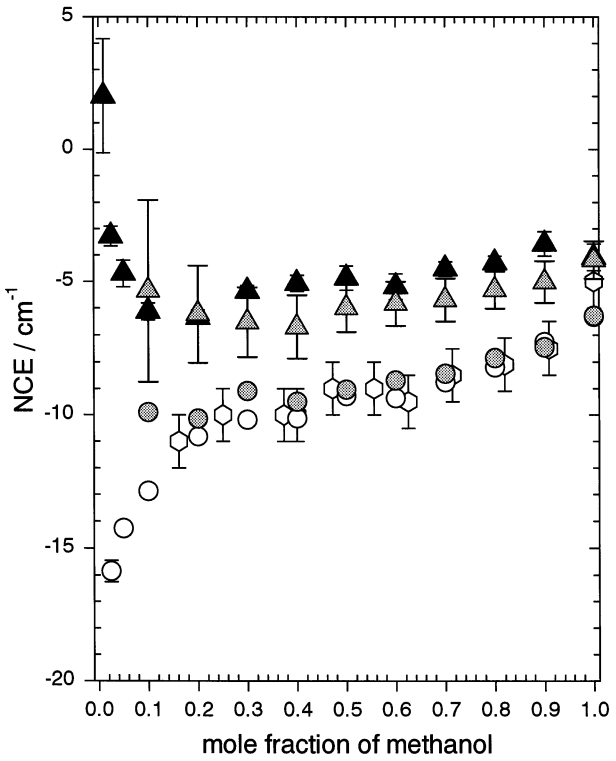

Figure 7. Observed and simulated dependence of the Raman noncoincidence effect of the C−O stretching band of methanol on the mole fraction of methanol in CCl_4 at 293 K. NCE_p is determined from the peak frequencies $\tilde{\nu}_{peak}$, and NCE_M from the first moments M_1. Circle (○): NCE_p; upward triangle (△): NCE_M. The open and filled symbols denote observed values, and the shaded symbols denote simulated values. The hexagons denote the values of NCE_p observed in ref 9.

a very weak trace of this end-of-chain ν(O−H) band can be detected, in accordance with the IR spectrum[36] of neat liquid methanol.

For the anisotropic component also, the peak frequency and the shape of the oligomer band at ∼3380 cm^{-1} do not appreciably change with dilution, but the first moment shows a slight and gradual increase starting at $x_m \sim 0.5$ due to the increasing intensity of the narrow band attributed to the end-of-chain ν(O−H). The latter also shifts from 3640(3) cm^{-1} to 3645.7(7) cm^{-1} with dilution (close to the position measured by IR spectroscopy,[36] 3644(1) cm^{-1}), although without any clear evidence of narrowing.

The MD results for the shift of the peak frequencies and the first moments are in reasonable agreement with the Raman spectroscopic results at least until down to $x_m = 0.5$. The increasing quantitative deviation between experimental and MD results at lower concentrations is due to the fact that at the present stage the MD simulation is not able to reproduce the strong increase of the end-of-chain O−H band intensity (see Figure 3).

B. Noncoincidence Effect. The concentration dependence of the NCE obtained from the peak frequencies (NCE_p) and from the first moments (NCE_M) of the ν(C−O) band is shown in Figure 7. It is seen that the observed value of NCE_p changes from −5.0(1) cm^{-1} in neat liquid to −13.0(2) cm^{-1} at $x_m = 0.1$. This result is quantitatively well reproduced by the MD simulation and is in agreement with the results of ref 9.

More importantly, both in the experiment and in the MD simulation the NCE_M of the ν(C−O) mode [experimentally $NCE_M = -4.1(5)$ cm^{-1} at $x_m = 1.0$] becomes more *negative* upon dilution in CCl_4 down to $x_m \sim 0.2$ [where $NCE_M = -6.3(2)$ cm^{-1}]. Only below this concentration there is a reversal of tendency, until NCE_M approaches zero at high dilution ($x_m \leq 0.02$). The increase of the magnitude of NCE with dilution is opposed to the usual behavior[4,20] observed with polar non-hydrogen-bonded liquids diluted in either nonpolar or polar solvents.

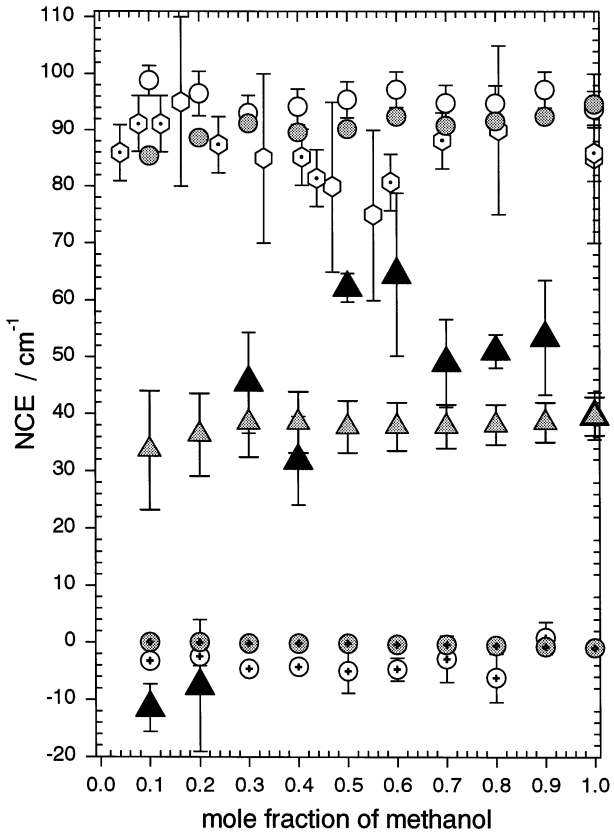

Figure 8. Observed and simulated dependence of the Raman noncoincidence effect of the O−H stretching band of methanol on the mole fraction of methanol in CCl_4 at 293 K. NCE_p is determined from the peak frequencies $\tilde{\nu}_{peak}$, and NCE_M from the first moments M_1. Circle (○): NCE_p; upward triangle (△): NCE_M. The open and filled symbols denote observed values, and the shaded symbols denote simulated values. The symbols with plus (+) at the center denote the values for the end-of-chain band. The open and dotted hexagons denote the values of NCE_p observed in refs 9 and 10, respectively.

The result that the magnitude of NCE_p is larger than that of NCE_M is mainly due to the red-tailed asymmetry of the isotropic Raman band. Based on Knapp's model,[24] this band asymmetry is reasonably explained by intermolecular resonant vibrational interactions, which are predominantly distributed around positive values (leading to negative NCE). It is thus not necessarily due to hot bands as discussed in ref 7.

The concentration dependence of the noncoincidence effect (NCE_p and NCE_M) of the ν(O−H) band is shown in Figure 8. It is seen that there is reasonably quantitative agreement between the experimental and MD simulation results. For the value of NCE_p, in which only the broad ν(O−H) band is involved, our results are in good agreement with those obtained in refs 9 and 10. Within the experimental and statistical (computational) uncertainties, this value is essentially independent of concentration [$NCE_p = 94(3)$ cm^{-1} at $x_m = 1.0$ and 99(3) cm^{-1} at $x_m = 0.1$]. The value of NCE_M [$NCE_M = 39(4)$ cm^{-1} at $x_m = 1.0$] also remains large upon dilution in CCl_4 down to $x_m = 0.3$ (where $NCE_M = 45.5(8.9)$ cm^{-1}). Further dilution leads to a decrease of NCE_M due to the increasing intensity of the end-of-chain ν(O−H) band. This narrow band also shows a small

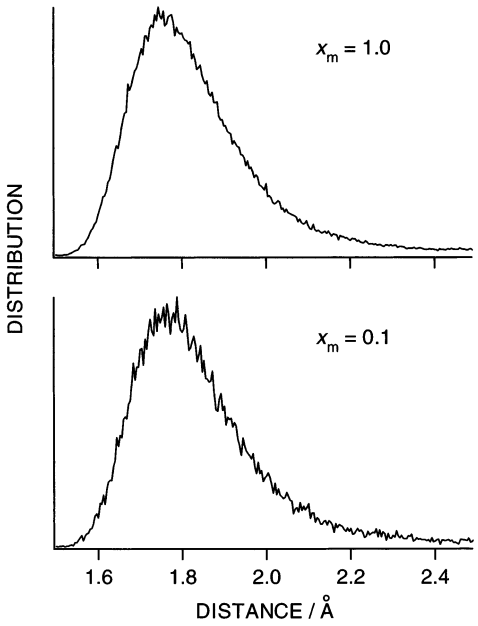

Figure 9. Calculated distributions of the O···H hydrogen-bond length $r_{O\cdots H}$ in neat liquid methanol ($x_m = 1.0$) and in a methanol−CCl_4 mixture at $x_m = 0.1$.

NCE ($NCE_p = -6.2(4.0)$ cm^{-1} at $x_m = 0.8$), but with the sign opposite to that of the oligomer ν(O−H) band. This NCE decreases to $NCE_p = -3.2(1.2)$ cm^{-1} at $x_m = 0.1$. The MD results for this band show the NCE of the correct sign ($NCE_p = -1.0$ cm^{-1} at $x_m = 1.0$), although they somewhat underestimate the magnitude. Presently there is no interpretation for the origin of this NCE, but its appearance may confirm that this narrow band contains contributions of the free OHs of hydrogen-bonded chains in addition to solvated monomers.[37]

The result that the value of NCE_p is larger than NCE_M for the oligomer ν(O−H) band is due to the strongly blue-tailed asymmetry of the isotropic Raman band. As discussed in Section 2C, the diagonal force constant of the ν(O−H) mode, the square root of which is proportional to the intrinsic vibrational frequency of the O−H oscillator (i.e., the frequency when the intermolecular resonant vibrational interaction is switched off), is related to the O···H hydrogen-bond length $r_{O\cdots H}$, which manifests the hydrogen-bond strength. The distributions of $r_{O\cdots H}$ obtained in the present MD simulations for $x_m = 1.0$ and 0.1 are shown in Figure 9. It may be reasonable to consider that the profile of the oligomer ν(O−H) band reflects the form of this distribution of $r_{O\cdots H}$, taking into account that the asymmetry of the band profile and the form of the distribution of $r_{O\cdots H}$ are both essentially independent of concentration in the range of $1.0 \geq x_m \geq 0.1$. Based on Knapp's model,[24] band asymmetry also arises from intermolecular resonant vibrational interactions between ν(O−H) oscillators. Since the coupling constants are negative (leading to positive NCE), this mechanism also gives rise to blue-tailed asymmetry.

C. Relation between the Noncoincidence Effect and Liquid Structures. To examine the contribution of interacting molecules to NCE as a function of intermolecular distance, the pair distribution functions[19,20b,38] $g(\boldsymbol{R}_{ij}; \boldsymbol{\Omega}_i, \boldsymbol{\Omega}_j)$ of the OH and CO bonds are evaluated by expanding them to the second order as

$$g(\boldsymbol{R}_{ij}; \boldsymbol{\Omega}_i, \boldsymbol{\Omega}_j) = g_0(R_{ij}) + h_\Delta(R_{ij})\boldsymbol{\Omega}_i\boldsymbol{\Omega}_j + h_D(R_{ij})\,[3(\boldsymbol{R}_{ij}\boldsymbol{\Omega}_i)(\boldsymbol{R}_{ij}\boldsymbol{\Omega}_j)/R_{ij}^2 - \boldsymbol{\Omega}_i\boldsymbol{\Omega}_j] \quad (1)$$

where $\boldsymbol{R}_{ij}$ is the vector connecting the relevant (OH or CO) bonds of molecules i and j, R_{ij} is the length of this vector, and $\boldsymbol{\Omega}_i$ and $\boldsymbol{\Omega}_j$ are the unit vectors in the direction of the relevant bonds of the two molecules. In the case where this second-order expansion is a good approximation of $g(\boldsymbol{R}_{ij}; \boldsymbol{\Omega}_i, \boldsymbol{\Omega}_j)$, NCE_M is proportional to $H_D(\infty)\ \rho\ x_m^{-1}$,[4] where ρ is the total number density and the function $H_D(r)$ is defined as

$$H_D(r) = \int_0^r \mathrm{d}R\ h_D(R)/R \quad (2)$$

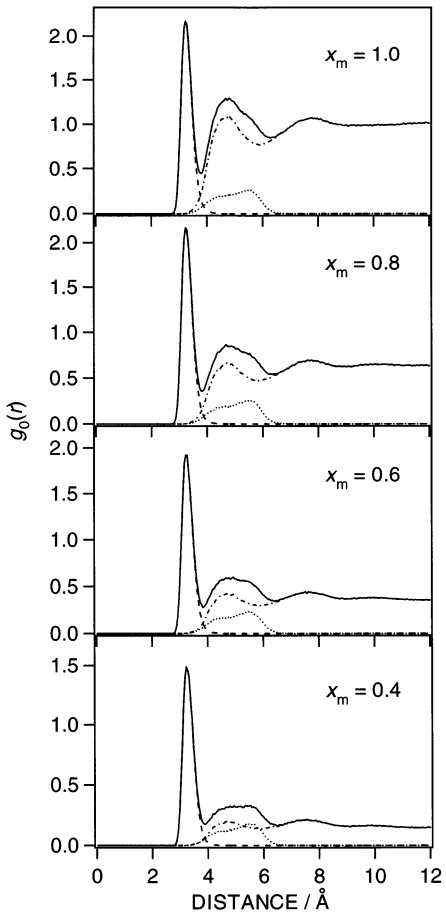

Figure 10. Pair distribution function [zeroth-order component, $g_0(r)$] of the CO bonds calculated for neat liquid methanol ($x_m = 1.0$) and methanol/CCl_4 mixtures at $x_m = 0.8$, 0.6, and 0.4, normalized so that $g_0(r) \rightarrow x_m^2$ as $r \rightarrow \infty$. Solid line: total profiles; dashed line: contribution from molecule pairs that are directly hydrogen bonded to each other (class 1); dotted line: contribution from molecules that are not directly hydrogen bonded to each other but hydrogen bonded to a common molecule (class 2); dot−dashed line: contribution from "all the other" pairs of molecules (class 3).

In addition to the total profiles of these functions, as shown in Figures 3 and 4 of ref 19 for neat liquid methanol, the contributions of the following three classes of molecule pairs are calculated in the present study: (1) molecule pairs which are directly hydrogen bonded to each other, (2) molecule pairs which are *not* directly hydrogen bonded to each other but hydrogen bonded to a common molecule, and (3) all the other pairs of molecules, such as the pairs of molecules belonging to different hydrogen-bonded chains.

The functions $g_0(r)$ and $H_D(r)$ calculated for the CO bonds of methanol for $x_m = 1.0$, 0.8, 0.6, and 0.4 are shown in Figures 10 and 11. These functions are normalized so that $g_0(r) \rightarrow x_m^2$ as $r \rightarrow \infty$ (in this sense, they are equal to the functions denoted as $g_0'(r)$ and $H_D'(r)$ in our previous study[20b]). The form of $g_0(r)$ at $x_m = 1.0$ is quite similar to that of the radial distribution

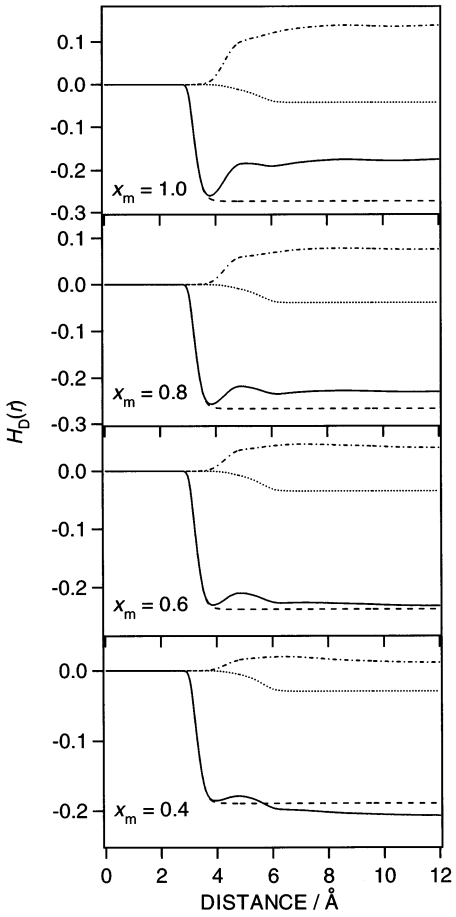

Figure 11. Pair distribution function [second-order component integrated, $H_D(r)$] of the CO bonds calculated for neat liquid methanol (x_m = 1.0) and methanol/CCl_4 mixtures at x_m = 0.8, 0.6, and 0.4. See also the caption for Figure 10.

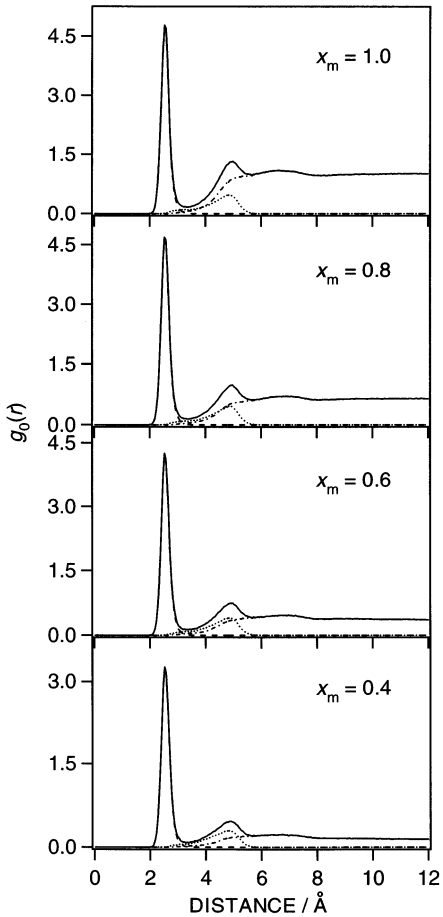

Figure 12. Pair distribution function [zeroth-order component, $g_0(r)$] of the OH bonds calculated for neat liquid methanol (x_m = 1.0) and methanol/CCl_4 mixtures at x_m = 0.8, 0.6, and 0.4. See also the caption for Figure 10.

function for the center of mass shown in a previous study,[39] since the center of the CO bond is located close to the center of mass in a methanol molecule.

As discussed in ref 19 for x_m = 1.0, it is seen that $H_D(r)$ overshoots the value of $H_D(\infty)$ at $r \cong 4$ Å, and a value nearly equal to $H_D(\infty)$ is reached at $r \cong 5$ Å. This is mainly due to partial cancellation of the contributions from molecule pairs belonging to classes 1 and 3. The molecule pairs belonging to class 1 are located in the $r < 4$ Å region (as shown by $g_0(r)$ in Figure 10), and give rise to the large negative value of $H_D(r)$ at $r \cong 4$ Å shown in Figure 11. In the $r > 4$ Å region this negative value is partially canceled by the positive contribution from the molecule pairs belonging to class 3. As discussed in ref 19 (see Table 1 and Figure 2 there), the different signs of the contributions to $H_D(r)$ result from the different signs of the coupling constants involved.

As methanol is diluted in CCl_4, the contribution from class 1 (if $H_D(r)$ shown in Figure 11 is multiplied by $\rho\, x_m^{-1}$) remains almost the same, since the number of molecule pairs belonging to class 1 that gives rise to the first peak of $g_0(r)$ at $r \cong 3.2$ Å does not decrease so much upon dilution, as shown in Figure 10 (this persistence of hydrogen bonds of methanol upon dilution in CCl_4 has also been shown in a previous MD simulation study[13]). The contribution from class 3 decreases upon dilution, because the number of molecule pairs belonging to this class decreases as hydrogen-bonded chains get separated from each other by the solvent molecules. As a result, the contribution from class 1 molecules gets predominant in dilute solutions. This kind of unbalanced, locally anisotropic change in the liquid structure leads to the increase of the negative NCE of the ν(C−O) band and is the reason for its apparently peculiar behavior.

It should be remarked here that NCE in methanol is affected by pressure as well as by methanol concentration. An increase in pressure results in a reduced magnitude of NCE_M of the ν(C−O) band,[7] because the increase in the number density induced by this thermodynamic change gives rise to a locally anisotropic variation in the liquid structure where only the number density of non-hydrogen-bonded pairs of closely located molecules, whose CO stretching vibrations are positively coupled, becomes larger.[18] It is thus concluded that the effects of pressure and methanol concentration on the NCE may be interpreted in a consistent way, since such a locally anisotropic variation in the liquid structure is induced by a change in either of these two variables. In other words, a reduced magnitude of NCE observed at a high pressure (for neat liquid methanol) is qualitatively interpreted as if the concentration dependent behavior is extended into the "$x_m > 1$" region, in the sense that non-hydrogen-bonded pairs of molecules are located closer to each other than in the $x_m = 1$ liquid at ambient pressure.

The functions $g_0(r)$ and $H_D(r)$ calculated for the OH bonds of liquid methanol are shown in Figures 12 and 13 for x_m = 1.0, 0.8, 0.6, and 0.4. In this case, a large part of $H_D(\infty)$ is explained by the contribution from class 1 in the $r < 3$ Å region, which remains almost the same upon dilution. The contributions from the other classes are very small.[19] It may be said, therefore, that the almost constant values of the NCE obtained for the OH stretching band in the $0.4 \leq x_m \leq 1$ range indicate

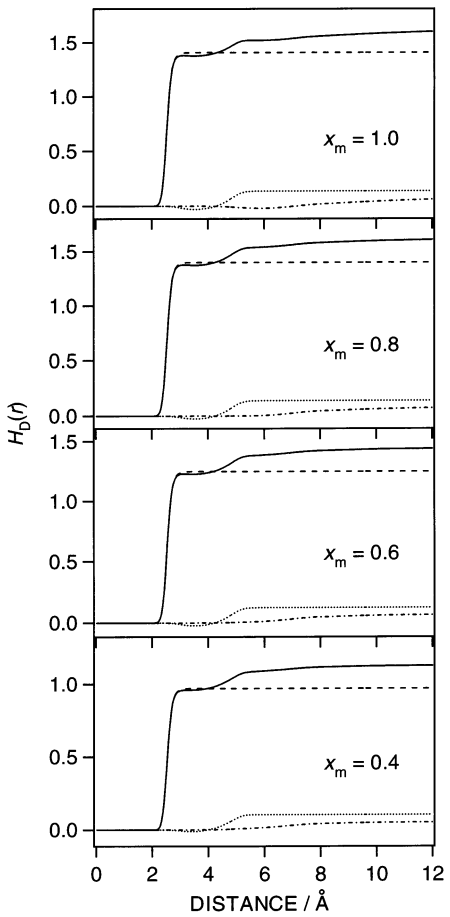

Figure 13. Pair distribution function [second-order component integrated, $H_D(r)$] of the OH bonds calculated for neat liquid methanol ($x_m = 1.0$) and methanol/CCl_4 mixtures at $x_m = 0.8$, 0.6, and 0.4. See also the caption for Figure 10.

persistence of hydrogen bonds upon dilution of methanol in CCl_4, in accord with the result of a previous MD simulation study.[13]

4. Conclusions

The main conclusions obtained in the present study may be summarized as follows. (1) The magnitude of the negative NCE observed for the ν(C−O) band increases upon dilution of methanol in CCl_4 down to $x_m \sim 0.2$, while the positive NCE of the ν(O−H) band remains almost the same upon dilution down to $x_m \sim 0.3$. (2) The experimental and MD simulations results are in agreement with each other in this respect. The parametrization adopted in the simulations is therefore considered to be reasonable. However, it should also be remarked that the strong increase of the end-of-chain ν(O−H) band that occurs upon dilution down to $x_m < 0.2$ could not be well reproduced at the present stage. (3) It is clarified by the MD simulations that a locally anisotropic change in the liquid structure that occurs upon dilution, where many molecules remain to be hydrogen bonded but hydrogen-bonded chains get separated from each other, is the main reason for the observed behavior of the NCE. (4) The result that the magnitude of NCE_p is larger than that of NCE_M is mainly due to the asymmetry of the isotropic Raman band. For the ν(C−O) band, the asymmetry is reasonably explained by Knapp's model,[24] in which intermolecular resonant vibrational interaction is involved. For the ν(O−H) band, an asymmetric distribution of the O···H hydrogen-bond lengths seems to be also important.

As described above, the apparently peculiar behavior of the NCE that occurs upon dilution of methanol in CCl_4 is due to a locally anisotropic change in the liquid structure. The NCE is sensitive to such a local anisotropy of liquid structure because it is related to the integrated second-order term $H_D(r)$ of the expansion of pair distribution function $g(\boldsymbol{R}_{ij}; \boldsymbol{\Omega}_i, \boldsymbol{\Omega}_j)$ shown in eqs 1 and 2. It may be said that this is a distinctive feature of the NCE among various quantities that can be analyzed in liquid structure studies.

Acknowledgment. This study was partially supported by a Grant-in-Aid for Scientific Research from the Ministry of Education, Culture, Sports, Science, and Technology of Japan (for H.T.). M.M. thanks Franco Aliotta and Marco Pieruccini, IPCF CNR Messina, for fruitful discussions.

References and Notes

(1) Fini, G. C.; Mirone, P.; Fortunato, B. *J. Chem. Soc., Faraday Trans. 2* **1973**, *69*, 1243.

(2) (a) Wang, C. H.; McHale, J. L. *J. Chem. Phys.* **1980**, *72*, 4039. (b) McHale, J. L. *J. Chem. Phys.* **1981**, *75*, 30. (c) Mirone, P. *J. Chem. Phys.* **1982**, *77*, 2704. (d) McHale, J. L. *J. Chem. Phys.* **1982**, *77*, 2705.

(3) (a) Döge, G.; Schneider, D.; Morresi, A. *Mol. Phys.* **1993**, *80*, 525. (b) Schneider, T. Ph.D. thesis, Technical University Braunschweig, 1993.

(4) Logan, D. E. *Chem. Phys.* **1989**, *131*, 199, and references therein.

(5) NIST Chemistry Webbook: http://webbook.nist.gov/.

(6) Miani, A.; Hånninen, V.; Horn, M.; Halonen, L. *Mol. Phys.* **2000**, *98*, 1737.

(7) (a) Zerda, T. W.; Thomas, H. D.; Bradley, M.; Jonas, J. *J. Chem. Phys.* **1987**, *86*, 3219. (b) Thomas, H. D.; Jonas, J. *J. Chem. Phys.* **1989**, *90*, 4632.

(8) Bertie, J. E.; Michaelian, K. H. *J. Chem. Phys.* **1998**, *109*, 6764.

(9) (a) Kecki, Z.; Sokolowska, A.; Yarwood, J. *J. Mol. Liquids* **1999**, *81*, 213. (b) Sokolowska, A. *J. Raman Spectrosc.* **1999**, *30*, 507.

(10) (a) Perchard, C.; Perchard, J. P. *J. Raman Spectrosc.* **1975**, *3*, 277; **1978**, *7*, 173. (b) Maillard, D.; Perchard, C.; Perchard, J. P. *J. Raman Spectrosc.* **1978**, *7*, 178.

(11) Haugney, M.; Ferrario, M.; McDonald, I. R. *J. Phys. Chem.* **1987**, *91*, 4934; *Mol. Phys.* **1986**, *58*, 849.

(12) Svishchev, I. M.; Kusalik, P. G. *J. Chem. Phys.* **1994**, *100*, 5165.

(13) Veldhuizen, R.; de Leeuw, S. W. *J. Chem. Phys.* **1996**, *105*, 2828.

(14) Padró, J. A.; Saiz, L.; Guàrdia, E. *J. Mol. Struct.* **1997**, *416*, 243.

(15) Shilov, I. Y.; Rode, B. M.; Durov, V. A. *Chem. Phys.* **1999**, *241*, 75.

(16) Bakó, I.; Jedlovszky, P.; Pálinkás, G. *J. Mol. Liquids* **2000**, *87*, 243.

(17) Durov, V. A.; Shilov, I. Yu. *J. Mol. Liquids* **2001**, *92*, 165.

(18) Torii, H.; Tasumi, M. *J. Chem. Phys.* **1993**, *99*, 8459.

(19) Torii, H. *J. Phys. Chem. A* **1999**, *103*, 2843.

(20) (a) Musso, M.; Giorgini, M. G.; Döge, G.; Asenbaum, A. *Mol. Phys.* **1997**, *92*, 97. (b) Torii, H.; Musso, M.; Giorgini, M. G.; Döge, G. *Mol. Phys.* **1998**, *94*, 821.

(21) Musso, M.; Torii, H.; Giorgini, M. G.; Döge, G. *J. Chem. Phys.* **1999**, *110*, 10076.

(22) Giorgini, M. G.; Musso, M.; Ottaviani, P. *Mol. Phys.* **2001**, *99*, 1485.

(23) Giorgini, M. G.; Musso, M.; Asenbaum, A.; Döge, G. *Mol. Phys.* **2000**, *98*, 783.

(24) Knapp, E. W. *J. Chem. Phys.* **1984**, *81*, 643.

(25) Knapp, E. W.; Fischer, S. F. *J. Chem. Phys.* **1982**, *76*, 4730.

(26) Kabisch, G.; Pollmer, K. *J. Mol. Struct.* **1982**, *81*, 35.

(27) NIST Atomic Spectra Database: http://physics.nist.gov/.

(28) Gao, J.; Habibollazadeh, D.; Shao, L. *J. Phys. Chem.* **1995**, *99*, 16460.

(29) Chang, T.-M.; Peterson, K. A.; Dang, L. X. *J. Chem. Phys.* **1995**, *103*, 7502.

(30) To do meaningful simulations for more dilute solutions, the simulations box should be enlarged to include a sufficiently large number of methanol molecules. However, the use of polarizable potential functions has made those simulations prohibitively expensive at present.

(31) Frisch, M. J.; Trucks, G. W.; Schlegel, H. B.; Scuseria, G. E.; Robb, M. A.; Cheeseman, J. R.; Zakrzewski, V. G.; Montgomery, J. A., Jr.; Stratmann, R. E.; Burant, J. C.; Dapprich, S.; Millam, J. M.; Daniels, A. D.; Kudin, K. N.; Strain, M. C.; Farkas, O.; Tomasi, J.; Barone, V.; Cossi, M.; Cammi, R.; Mennucci, B.; Pomelli, C.; Adamo, C.; Clifford, S.;

Ochterski, J.; Petersson, G. A.; Ayala, P. Y.; Cui, Q.; Morokuma, K.; Malick, D. K.; Rabuck, A. D.; Raghavachari, K.; Foresman, J. B.; Cioslowski, J.; Ortiz, J. V.; Baboul, A. G.; Stefanov, B. B.; Liu, G.; Liashenko, A.; Piskorz, P.; Komaromi, I.; Gomperts, R.; Martin, R. L.; Fox, D. J.; Keith, T.; Al-Laham, M. A.; Peng, C. Y.; Nanayakkara, A.; Gonzalez, C.; Challacombe, M.; Gill, P. M. W.; Johnson, B. G.; Chen, W.; Wong, M. W.; Andres, J. L.; Head-Gordon, M.; Replogle, E. S.; Pople, J. A. *Gaussian 98*; Gaussian, Inc.: Pittsburgh, PA, 1998.

(32) When $r_{O\cdots H}$ is long enough, the values of f_{OH} and/or $(\partial\mu/\partial Q)_{OH}$ obtained by the formulas overshoot the values for molecules without a hydrogen-bonded OH group. For such molecules, we adopted the latter values as f_{OH} and/or $(\partial\mu/\partial Q)_{OH}$.

(33) (a) Eysel, H. H.; Bertie, J. E. *J. Mol. Struct.* **1986**, *142*, 227. (b) Bertie, J. E.; Zhang, S. L.; Eysel, H. H.; Baluja, S.; Ahmed, M. K. *Appl. Spectrosc.* **1993**, *47*, 1100.

(34) (a) Staib, A. *J. Chem. Phys.* **1998**, *108*, 4554. (b) Meyer zum Büschenfelde, D.; Staib, A. *Chem. Phys.* **1998**, *236*, 253.

(35) Buck, U.; Siebers, J.-G. *J. Chem. Phys.* **1998**, *108*, 20.

(36) Kristiansson, O. *J. Mol. Struct.* **1999**, *477*, 105.

(37) The end-of-chain O−H stretching band of liquid octanol also shows a negative NCE of comparable magnitude. Morresi, A., private communication.

(38) Blum, L. *J. Chem. Phys.* **1972**, *57*, 1862.

(39) Chalaris, M.; Samios, J. *J. Phys. Chem. B* **1999**, *103*, 1161.